

Article

# Archaeometric Analysis of the Objects from the Scala Santa (Holy Stairs) in the Crypt under the Piarist Church in Cracow (Poland)

Mariola Marszałek <sup>1,\*</sup> , Adam Gawel <sup>1</sup>, Karolina Pachuta <sup>2</sup> and Eliza Buszko <sup>2</sup>

<sup>1</sup> Department of Mineralogy, Petrography and Geochemistry, AGH University of Science and Technology, 30-059 Kraków, Poland; agawel@agh.edu.pl

<sup>2</sup> Conservation and Renovation Firm Piotr Białko Ltd., 30-608 Kraków, Poland; kpachuta@fkpb.pl (K.P.); ebuszko@fkpb.pl (E.B.)

\* Correspondence: mmarszal@agh.edu.pl

**Abstract:** Conservators extracted and preserved reliquaries hidden in the steps of the right flight of the Holy Stairs erected in the Piarist church crypt in Cracow (Poland). Three items from among 59 reliquaries were selected for specialist analyses: a framed, transparent cross containing a particle of the True Cross, and two opaque beads; an ornamented blue one without a hole and a drilled black one were analysed using non-destructive and non-invasive methods. The methods included scanning electron microscopy coupled with energy dispersive X-ray spectrometry, Raman microspectroscopy and X-ray diffractometry. The reliquary cross was found to be made of rock crystal and framed with an alloy of gold, silver and probably copper. The beads are made of glass; the blue bead represents forest plant-ash potash–lime glass and the black one, plant-ash soda–lime glass. Cobalt, probably along with copper, was used to produce the colour of the blue bead; manganese and iron ions were used to produce that of the black bead. Lead was present in both beads as one of the minor components and also as a component of corrosion products on their surfaces and probably also as part of the filler for the ornamentation of the blue bead. Nevertheless, it cannot be ruled out that the lead compounds were introduced intentionally to emphasize the bead ornamentation. The possible place and date of manufacture of the artefacts were also discussed.

**Keywords:** Scala Santa; Piarist Church; Cracow; Poland; glass beads; reliquary cross; rock crystal; non-destructive methods



**Citation:** Marszałek, M.; Gawel, A.; Pachuta, K.; Buszko, E. Archaeometric Analysis of the Objects from the Scala Santa (Holy Stairs) in the Crypt under the Piarist Church in Cracow (Poland). *Minerals* **2021**, *11*, 1179. <https://doi.org/10.3390/min11111179>

Academic Editor: Domenico Miriello

Received: 24 September 2021

Accepted: 20 October 2021

Published: 25 October 2021

**Publisher's Note:** MDPI stays neutral with regard to jurisdictional claims in published maps and institutional affiliations.



**Copyright:** © 2021 by the authors. Licensee MDPI, Basel, Switzerland. This article is an open access article distributed under the terms and conditions of the Creative Commons Attribution (CC BY) license (<https://creativecommons.org/licenses/by/4.0/>).

## 1. Introduction

The Piarist church in Cracow represents one of the finest examples of Baroque art in Poland [1]. The church is located near the Main Square and is famous principally for its trompe-l'œil (illusionistic) polychrome paintings in the nave and chancel made by the prominent Moravian painter Franz Eckstein in 1727 and 1733 [2]. The crypt under the church, where the Holy Sepulchre was traditionally arranged, was also used as a funeral chapel [3]. In the period of Martial Law (1981–1983), it hosted independent artists and meetings of the anti-communist opposition. The Sacred Art Centre and the renowned “Piarist Crypt” art gallery have operated in the lower church since 1997 [4].

The gallery had to be adapted to the requirements of today's art exhibitions and thus conservatory repair was initiated in the lower church. Numerous sensational discoveries were made during the work, such as Baroque frescoes, catacombs [5], and 59 reliquaries in mysterious stairs in the crypt chancel. As the conservatory and research project progressed, it became clear that the crypt under the church was originally designed as a chapel of the Holy Stairs, a unique historical object in world terms (Figure 1).



**Figure 1.** A general view of the Holy Stairs in the monastery of the Piarists in Cracow. Condition following conservatory work in 2017–2020.

The extraordinary opportunity presented by the conservation work and the “rediscovery” of the Holy Stairs provided a unique possibility to analyse the objects within. No works on a similar subject have been found in the available literature.

The reliquaries and their heterogeneous contents discovered were analysed by an interdisciplinary team of scientists, including art conservators, historians, chemists, geologists, anthropologists, botanists, and experts in examining fabrics and paper [6]. This study contains conclusions concerning three items of particular interest. Research conducted in the church clearly demonstrated that the relics found in the Holy Stairs, including particles of the True Cross, represented the most valuable religious objects that gave the Cracow chapel special importance and emphasised its uniqueness.

### 1.1. History of the Holy Stairs

The Scala Santa is an ideal copy of the stairs in the Antonia Fortress of Jerusalem. According to the Bible and Christian tradition, Christ, scourged and crowned with thorns, ascended the Stairs to appear before Pilate and was sentenced to death there. Legend has it that the original stairs (28 steps made from Tyrian marble) were found in Jerusalem in 326 by Saint Helena and transported to Rome at her request. They were installed in the papal palace to form the main, celebratory staircase. When Pope Gregory XI returned to Rome in 1377, the old buildings were in extremely poor condition and consequently, the main seat of the papacy was moved to the Vatican hill.

On the eve of the jubilee year of 1450, the main stairs in the old palace were demonstrated to the faithful as the stairs from the praetorium of Pilate, stained with drops of Jesus Christ’s blood. Relics were placed in the stairs no later than in the 15th century, and step 11 was marked with a metallic cross and grid to protect supposed blood traces. Legend has it that Jesus heard the sentence and fell on that step. The stairs became a cult object and may only be climbed on one’s knees since then.

Pope Sixtus V ordered the demolition of the old palace and the construction of a new one designed as his summer residence in 1589. Domenico Fontana was assigned to carry out the project. The new, early Baroque chapel of the Holy Stairs was profoundly revered by the faithful and pilgrims. Pope Innocent III ordered that the steps, gouged by pilgrims’ knees, be encased in wood in 1723 [7].

The Holy Stairs were copied as of the early 17th century, initially in Italy, then in the Habsburg Empire and other Roman Catholic states in Europe. The most renowned objects of this type in modern-day Poland include the stairs at Pilate’s Hall in Kalwaria Zebrzydowska dating back to 1630 [8] and the chapel in Sońnica, built in 1776 [9].

The chapel of Holy Stairs in the crypt of the Piarist church in Cracow was financed by Father Stefan Dembiński and consecrated in 1733 [10]. Its unusual architecture, distin-

guished by its outstanding artistic values, was probably designed by Kacper Bażanka. It was designed together with the sanctuary as a whole and occupies the entire lower church, constituting its idealistic foundation [11].

The Cracow Holy Stairs are monumental, consisting of two flights, and occupy the entire chancel of the chapel. The right flight of 26 low steps and two landings (totalling the required number of 28) is made from compacted limestone, replacing marble; the faithful ascended it on their knees, uttering special prayers. The left flight of 23 steps is made from sandstone and designed for normal descent. At the top of the stairs, the altar of Christ's Prison was located. A cave designed to host the Holy Sepulchre was located under the stairs [12].

Baroque forms of piety and the original function of the space gradually faded away in the late 19th century [13]. The cave under the stairs was destroyed during repair and electrification of the crypt in 1983–1984. No documentation of work done at that time has been preserved [14]. The reliquaries hidden in the steps were forgotten. Their discovery in July 2018 was a major surprise and required verification of the programme and the entire concept of use of the lower church.

### *1.2. The Reliquaries from the Cracow Holy Stairs*

Archive records suggest that relics for the Cracow Holy Stairs were obtained by the Polish prince Jakub Ludwik Sobieski from Pope Benedict XIII prior to 1730 [15]. The relics probably included remains of saintly martyrs. They were placed in the risers of the right flight of stairs in carved openings filled with mortar. The openings were allocated symmetrically, two per step at its ends (Figure 2a–c). In the mid-18th century, the former provincial superior of the Piarists, Father Walenty Kamieński, obtained relics of the True Cross [16]. The precious particles were hidden in the central sections of the risers of steps 2, 11 and 28. The locations were not accidentally chosen: according to tradition, those steps were stained with drops of suffering Christ's blood and are marked with metallic crosses in the Roman chapel. Souvenirs from the Holy Land brought by Father Piotr Włost were added in later years [12].

Conservators found a total of 59 reliquaries or their remains in the right flight of the Holy Stairs. Unfortunately, no documents are preserved that would specifically describe the relics contained in the reliquaries.

Various types of relics are distinguished in Christianity. The classification was simplified in 2017 [17] and limited to two degrees: significant relics and non-significant relics. The first class includes the body of the blessed and of the saints or notable parts of the bodies themselves or the ashes obtained by their cremation. The second class includes little fragments of the body of the blessed and of the saints as well as objects that came in direct contact with their person. Mączyński and others claim [12,15] that the Piarist church hosts relics of saints, particles of the True Cross and souvenirs from the Holy Land (locations venerated by the Christians).

The reliquaries from the Cracow Holy Stairs located in the extreme openings at the step ends had similar shapes. Each of those reliquaries was designed as an iron casket in the form of a rectangular cuboid (Figure 2d). With a relic placed inside, it was filled with a fossil resin. The resin was meant to strengthen the structure of the casket and probably to inhibit corrosive processes. Each reliquary was wrapped in narrow strips of blue fabric secured using a red wax seal. The seals contained gypsum, vermilion and shellac. Despite the poor condition of the reliquaries (and the relics), certain repeated arrangement patterns of their contents were identified. Anthropologists and forensic experts identified 25 bone fragments (Figure 2e) representing non-significant relics. The relics were described on pieces of paper and then carefully wrapped in thin handmade ribbed paper shaped as a square or rectangle. The space between the paper and internal walls of a reliquary was filled with a material identified as cotton (Figure 2f) and other heterogeneous components, such as conifer needles and especially leaves, animal armours, and soil and gravel varying in grain size and colour. Soil scientists did not reveal any properties clearly indicating that the soil samples originated from outside

Cracow. However, an analysis of plant material demonstrated the presence of Lebanon cedar (or Atlas cedar), that is, a species from the Middle East. The most interesting relic was found in the central sections of step 11 (Figure 3a). According to the literature on the subject, this step contained relics of the True Cross. One of the openings (no. 24A) contained an aesthetically unique blue bead with an inlay relief decoration (Figure 3b). Opening no. 3A contained a small black bead (Figure 3c) [18].



**Figure 2.** A view of a fragment of the right flight of the Holy Stairs in the monastery of the Piarists in Cracow. Condition during conservatory work. (a) Right flight of stairs after the removal of contents from all openings. (b) Soiled mortar that masks opening no. 7A with relics. (c) Opening no. 7A with removed masking mortar. (d) Contents of a sample opening taken out from a riser. (e) A fragment of bone tissue from one of the reliquaries. (f) Paper used to wrap bone fragments and cotton material.



**Figure 3.** Items selected for detailed tests. (a) The reliquary cross from opening no. 11B. (b) The blue bead from opening no. 24A. (c) The black bead from opening no. 3A.

## 2. Materials and Methods

Three objects found in the steps of the Holy Stairs were examined: the reliquary cross from opening no. 11B, the blue bead from opening no. 24A and the black bead from opening no. 3A. The items were selected considering their outstanding aesthetic values compared to other components.

The reliquary cross (Figure 3a) is a small reliquary (about 5 cm high and less than 3 cm wide), in the form of a simple Latin cross with bevelled edges and a trapezoid cross-section. It consists of two main components: a base and a cover. Both are enclosed in a gilded metallic casing with openwork decoration. A shallow groove is in the middle of the base, containing a particle of the True Cross in the form of a smaller cross. The reliquary cross has an openwork filigree decoration. The edges of the cover are encircled by a narrow slat in the form of a simplified interlace. The upper part contains two members of a small hinge used to open the reliquary. A round protruding eye, a component of the lock, was found in the lower part of the cover. The other base part of the reliquary is also encircled by an interlace slat. The arms of the cross are also decorated with openwork forms resembling leaves or flowers. All consist of three round and thin overlapping petals, the middle one being slightly larger. Additionally, three narrow leaves with equal sizes and sharp ends are placed in each corner of the cross–arm intersection. The upper part contains the middle member of a hinge, and the base part contains a tongue used to close the reliquary. The small cross is well preserved. Its surface was soiled when taken out of the stairs. The hinges used to open the reliquary are characterised by a slight backlash. The filigree decoration is covered with local green deposits. A piece of thin twine originally threaded through the openwork decoration was also preserved. A wax seal of a bishop was originally attached to its end, affixed on a piece of paper with a detailed description of the relic. The description with the seal confirmed the origin and authenticity of the relic. Only traces of those components on the cross surface are preserved.

The vividly blue bead was removed from opening no. 24A (Figure 3b). It has the shape of a polygon with a slightly flattened face and a diameter of about one centimetre. The face of the bead was ground to obtain a square that has in its middle a shallow, currently slightly distorted engraving: a circle surrounded by small cavities with wavy external edges. It is filled with a white mix forming a kind of inlay. It has no hole. The bead is preserved in medium condition: it was heavily soiled when taken out of the stairs and small scratches are visible on its surfaces and losses in the white mix used to fill the relief.

The black bead has an oval shape and is about 4 mm wide (Figure 3c). It was found in opening 3A. It has a round hole in its middle, used to string it on thread or twine. The bead was preserved in very good condition. It was only superficially soiled when removed from the stairs.

The type of artefacts analysed placed significant limitations on the laboratory methods which could be applied during the investigation of the material. All artefacts were studied raw, without undergoing any preparation procedure and using non-destructive methods. Laboratory investigations were focused on mineralogical and geochemical analyses using scanning electron microscopy with energy dispersive spectrometry (SEM-EDS), X-ray diffractometry (XRD) and Raman microspectroscopy (RS).

The samples were studied using an FEI 200 Quanta FEG scanning electron microscope with an EDS/EDAX spectrometer (FEI Company, Fremont, CA, USA). The maximum excitation voltage was 20 kV and the pressure 60 Pa (the low vacuum mode). The samples were not coated.

In order to discover the phase composition of the studied objects, it was decided that the X-ray powder diffraction method (XRPD) should be used. It was understood that having equipment for powder preparations, the results would not be entirely satisfactory. However, an attempt was made in the hope that it would be possible to record even a few diffraction reflexes to allow phase identification. Considering that the specimens must not be physically altered in any way, a special holder was made to place the specimens securely in the measuring plane of the diffractometer. The XRD method requires the analysed surface to be flat and smooth. Unfortunately, in the case of the specimens studied, the choice of a suitable surface was very limited, and so, for the blue bead, X-ray patterns were recorded from the front (surface with ornamentation) and back surfaces, and for the cross from the front surface. There was no flat surface on the black bead. Its X-ray diffraction was thus recorded by placing its convex surface on the measuring plane of the instrument. Only the X-ray patterns of the blue bead were suitable for typical phase analysis. The values of interplanar distances were used to identify mineral phases, based on the data in the ICDD catalogue (Powder Diffraction File PDF-2. International Centre for Diffraction Data. 2018) and the XRAYAN computer program. A Rigaku Smart Lab 9.0 kW diffractometer with Cu-K $\alpha$  radiation was employed (RIGAKU Corporation, Tokyo, Japan). The diffractometer was equipped with a reflective graphite monochromator. The XRD patterns were recorded in the range of 2–75° 2 $\theta$  with the step size 0.05° 2 $\theta$ , counting time at 1 s/step at a voltage of 45 kV and a current of 200 mA.

The Raman spectra were recorded with a Thermo Scientific DXR Raman microscope with a 900 grooves/mm grating and a CCD detector (Thermo Scientific, Waltham, MA, USA). The Olympus 10 $\times$  (NA 0.25) and 50 $\times$  (NA 0.50) objectives (theoretical spot sizes 2.1  $\mu$ m and 1.1  $\mu$ m, respectively) were used. The sample was excited with a 532-nm laser. The laser power was selected to obtain spectra of the best quality and ranged from 3–10 mW (the maximum power is 10 mW). The spectra were recorded at the exposure time of 3 s and the number of exposures varied from 10 to 100. The spectra identification was performed using the RRUFF Raman Minerals spectral libraries as well as some data from the literature [19–25]. The band component analysis was undertaken using the Omnic software package, which enables the type fitting function to be selected and allows specific parameters to be fixed or varied accordingly. Band fitting was carried out using a Gauss–Lorentz cross-product function. For the fitting process, the minimum number of component bands were used. The symbols ‘s’, ‘m’ and ‘v’ used next to the position of the Raman bands describe their intensities (‘s’—strong, ‘m’—medium, ‘v’—very).

### 3. Results

#### 3.1. The Reliquary Cross from Opening No. 11B

The transparent, colourless material of the cross was examined. Since it was possible to open the cross, the analyses were also performed on its interior. We also checked the chemical composition of the metal frame along its arms.

The results of SEM-EDS analysis are shown in Figure 4 and Table 1 and the results of Raman microspectroscopy analysis performed on the transparent cross material, in Figure 5.

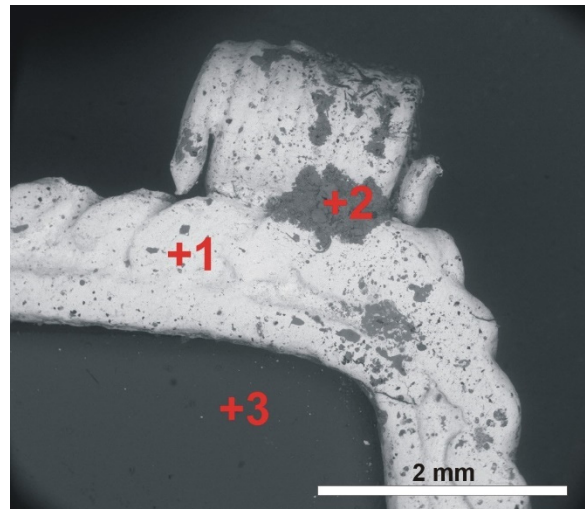


**Figure 4.** Backscattered electron (BSE) image of the cross. For chemical analyses obtained at the points numbered 1–3 see Table 1.

**Table 1.** Chemical composition, in weight percentage, of the material and frame of the cross. For the exact position of the analysed points, see Figure 4.

Elements	Analysed Points		
	+1	+2	+3
C	b.d.l.	11.72	b.d.l.
O	b.d.l.	42.88	48.53
Cl	b.d.l.	0.10	b.d.l.
Ag	53.41	2.12	b.d.l.
Cu	2.44	39.26	b.d.l.
Au	44.15	3.92	b.d.l.
Al	b.d.l.	b.d.l.	b.d.l.
Si	b.d.l.	b.d.l.	51.47
Total	100.00	100.00	100.00

b.d.l.—below detection limit.

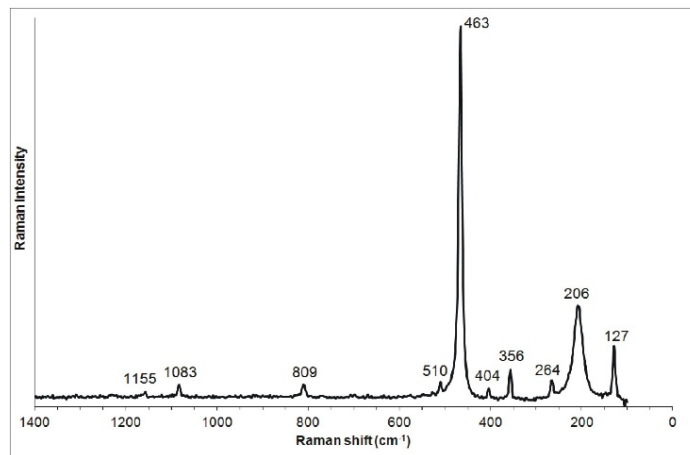


**Figure 5.** Representative characteristic Raman spectrum of the cross material.

EDS chemical analysis of the framing around the cross mainly showed the presence of gold Au (mean  $47.59 \pm 4.86$  wt%) and silver Ag (mean  $49.66 \pm 5.29$  wt %), copper Cu was found as an admixture (mean  $2.74 \pm 0.43$  wt%) (Figure 4, Table 1, point 1). Higher concentrations of Cu, being a result of corrosion, were only observed in a few places (Figure 4, Table 1, point 2). These concentrations were also visible to the naked eye, in the form of green granular clusters.

In the elemental composition (EDS) of the material from which the cross was made, only silicon Si and oxygen O were found (Figure 4, Table 1, point 3). This chemical composition suggests that it is quartz. The nature of this component has been conclusively confirmed using Raman microspectroscopy analyses and inferred from the bands at 127 (s), 206 (s), 264 (s), 356 (s), 404 (m), 463 (vs), 510 (m), 809 (m), 1083 (m), 1155 (m)  $\text{cm}^{-1}$ , related to Si-O vibrations [19] (Figure 5).

No reflections or diffraction effects characteristic of amorphous phases were observed in the cross material X-ray pattern. This is a typical feature of monocrystalline phases, in which the surface under study is not parallel to any of the lattice planes whose reflections would be observed in the measurement range. It can be concluded that the cross was cut out of the quartz (rock crystal) randomly, not in accordance with its natural planes.

### 3.2. The Blue Bead from Opening No. 24A

Both the top and bottom of the blue bead were examined. The white substance visible to the naked eye that fills the engraving on the surface of the bead (Figure 3b) was also analysed. It appeared to be relatively poorly bonded to the substrate. Microscopic (SEM) observations showed that in places it also covers other parts of the bead's surface, forming accumulations.

The results of chemical SEM-EDS analysis are shown in Figure 6, Table 2 and Figure 7, Table 3.

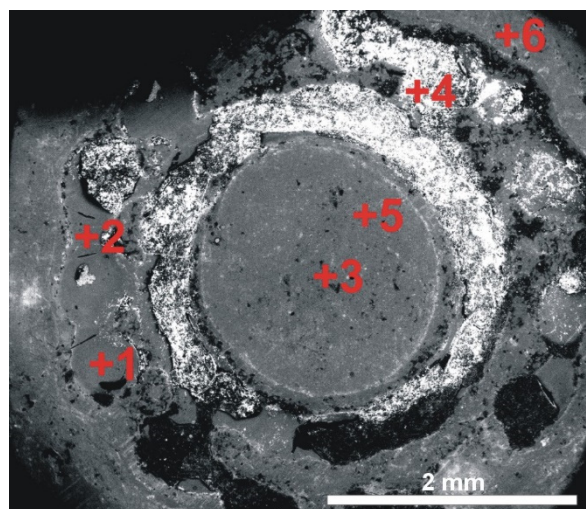


**Figure 6.** Backscattered electron (BSE) image of the blue bead surface with a white substance filling the bead ornamentation. For chemical analyses obtained at the points numbered 1–6, see Table 2.

**Table 2.** Chemical composition, in weight percentage, of the side of the blue bead with ornamentation. For all elements (except anion Cl), the composition is expressed as oxides weight %. The exact positions of the analysed points are shown in Figure 6.

	Analysed Points					
	+1	+2	+3	+4	+5	+6
CO <sub>2</sub>	b.d.l.	b.d.l.	42.82	25.31	b.d.l.	b.d.l.
F <sub>2</sub> O	b.d.l.	b.d.l.	b.d.l.	1.33	b.d.l.	b.d.l.
N <sub>2</sub> O <sub>5</sub>	b.d.l.	b.d.l.	b.d.l.	b.d.l.	b.d.l.	b.d.l.
Na <sub>2</sub> O	2.32	2.36	1.84	b.d.l.	2.48	2.19
MgO	0.72	0.39	0.41	b.d.l.	0.81	0.72
Al <sub>2</sub> O <sub>3</sub>	1.26	1.23	0.87	0.61	1.40	1.03
SiO <sub>2</sub>	71.68	73.48	39.51	3.31	69.50	70.24
P <sub>2</sub> O <sub>5</sub>	2.31	2.21	1.31	b.d.l.	2.46	1.89
SO <sub>3</sub>	0.27	b.d.l.	0.22	1.34	0.14	b.d.l.
PbO <sub>2</sub>	1.35	1.28	1.18	58.60	3.41	2.40
Cl	b.d.l.	b.d.l.	0.19	6.09	0.43	0.12
K <sub>2</sub> O	11.79	11.90	5.89	0.22	10.88	10.34
CaO	6.41	6.69	3.87	0.69	6.68	6.42
MnO	0.20	b.d.l.	0.15	0.33	0.09	0.53
Fe <sub>2</sub> O <sub>3</sub>	0.47	b.d.l.	0.26	b.d.l.	0.52	0.81
CoO	0.13	b.d.l.	0.19	0.49	0.21	0.74
NiO	0.40	b.d.l.	0.32	0.57	0.47	0.70
CuO	0.20	0.20	0.23	0.64	0.19	0.74
ZnO	0.49	0.26	0.73	0.47	0.34	1.13
Total	100.00	100.00	100.00	100.00	100.00	100.00

b.d.l.—below detection limit.

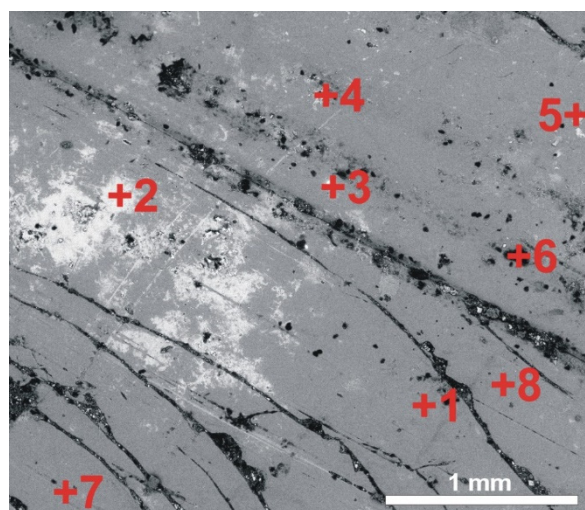


**Figure 7.** Backscattered electron (BSE) image of the underside surface of the blue bead. For chemical analyses obtained at the points numbered 1–8, see Table 3.

**Table 3.** Chemical composition, in weight percentage, of the underside of the blue bead. For all elements (except anion Cl) the composition is expressed as oxides weight %. The exact positions of the analysed points are shown in Figure 7.

	Analysed Points							
	+1	+2	+3	+4	+5	+6	+7	+8
CO <sub>2</sub>	b.d.l.	28.50	b.d.l.	49.08	39.08	77.49	b.d.l.	b.d.l.
N <sub>2</sub> O <sub>5</sub>	b.d.l.	b.d.l.	b.d.l.	b.d.l.	b.d.l.	11.52	b.d.l.	b.d.l.
Na <sub>2</sub> O	2.73	b.d.l.	1.79	0.99	b.d.l.	0.48	2.72	2.68
MgO	0.55	0.25	0.19	0.11	0.85	0.07	1.06	1.01
Al <sub>2</sub> O <sub>3</sub>	1.17	0.71	0.66	0.91	0.94	2.69	2.58	1.39
SiO <sub>2</sub>	72.22	35.85	53.25	12.74	30.97	4.04	70.86	72.16
P <sub>2</sub> O <sub>5</sub>	2.42	1.73	0.56	0.95	1.08	b.d.l.	2.51	2.50
ZrO <sub>2</sub>	b.d.l.	b.d.l.	b.d.l.	b.d.l.	b.d.l.	0.66	b.d.l.	b.d.l.
SO <sub>3</sub>	0.27	0.20	0.75	0.57	b.d.l.	0.51	b.d.l.	b.d.l.
PbO <sub>2</sub>	b.d.l.	0.17	29.40	2.24	b.d.l.	0.10	0.40	0.41
Cl	b.d.l.	0.59	0.24	5.02	0.22	0.52	b.d.l.	0.24
K <sub>2</sub> O	11.96	3.69	6.59	1.74	3.23	0.59	10.96	11.02
CaO	6.47	3.29	2.36	2.25	3.03	0.76	5.45	6.10
MnO	0.25	0.27	0.29	0.07	0.21	b.d.l.	b.d.l.	0.32
Fe <sub>2</sub> O <sub>3</sub>	0.25	0.27	0.76	0.49	0.75	0.05	0.79	0.56
CoO	0.24	0.17	0.48	b.d.l.	0.47	0.06	0.54	0.46
NiO	0.32	0.20	0.43	b.d.l.	0.61	0.07	b.d.l.	0.20
CuO	0.37	b.d.l.	0.39	11.72	1.99	0.11	0.58	0.60
ZnO	0.77	24.11	1.86	11.12	16.57	0.25	1.55	0.37
Total	100.00	100.00	100.00	100.00	100.00	100.00	100.00	100.00

b.d.l.—below detection limit.

EDS chemical analysis of the bead surface (with no additional accumulations clearly visible; Figure 6 and Table 2, points 1, 2, 5 and 6 and Figure 7, Table 3, points 1, 7 and 8) have mainly revealed the presence of Si (mean SiO<sub>2</sub>: 71.45 ± 0.48 wt%), K (mean K<sub>2</sub>O: 11.26 ± 0.58 wt%) and Ca (mean CaO: 6.32 ± 0.40 wt%) with an admixture of Na (mean Na<sub>2</sub>O: 2.50 ± 0.20 wt%). P (mean P<sub>2</sub>O<sub>5</sub>: 2.33 ± 0.21 wt%), Pb (mean PbO<sub>2</sub>: 2.01 ± 1.13 wt%), Al (mean Al<sub>2</sub>O<sub>3</sub>: 1.44 ± 0.48 wt%) and Mg (mean MgO: 0.75 ± 0.22 wt%) were also found at all analysed points. Additionally, elements such as Co, Cu, Zn, Mn, Fe and Ni were detected at almost all points. Their concentration is less than 1 wt%. C and S occur only rarely and are most likely associated with corrosion products (e.g., Figure 6 and Table 2, points 3 and 4 and Figure 7, Table 3, points 2–6).

EDS analysis of the white substance filling the decorative carving of the bead (Figure 6, Table 2, point 4), mainly showed the presence of lead (58.60 wt% PbO<sub>2</sub>); other components occurring in smaller quantities were carbon (25.31 wt% CO<sub>2</sub>) and chlorine (6.09 wt% Cl). Elements such as Si, K, Ca and Al that occur in smaller amounts not exceeding one wt% (with the exception of Si, ca. 3 wt% SiO<sub>2</sub>) came from the substrate. Analysis of the underside of the bead revealed, in places, the presence of a substance similar to that which fills the decorative carving on the surface. In addition to Pb, Zn and Cu were also found (Figure 7, Table 3, points 2–5).

The Raman spectra recorded from the surface of the bead shows two broad bands in the range of 200–1100 cm<sup>-1</sup> (Figure 8), suggesting the significantly amorphous nature of the substance (e.g., glass, opal; [20–22]). The broad band in the range of 200–700 cm<sup>-1</sup>, in which bands of 454, 534 and 598 cm<sup>-1</sup> were distinguished, can be associated with bending vibrations of Si-O-Si groups (characteristic for SiO<sub>4</sub> tetrahedra). The band around 1108 cm<sup>-1</sup> can be related to Si-O-Si stretching vibrations respectively. Additionally, the weak band in the range of 700–850 cm<sup>-1</sup> with the maximum of 794 cm<sup>-1</sup> and distinct band at 962 cm<sup>-1</sup> are present in all spectra. The former can be attributed to the symmetric Si-O-Si stretching vibration [21], the latter to the presence of PO<sub>4</sub><sup>3-</sup> groups [23,24]. This Raman spectrum suggests that the analysed material is glass, since the presence of two broad bands, with one centred at ca. 500 cm<sup>-1</sup> (SiO<sub>4</sub> tetrahedron bending modes) and the

other at ca.  $1000\text{ cm}^{-1}$  ( $\text{SiO}_4$  tetrahedron symmetrical stretching modes), is characteristic of this material (glass) [20,25].

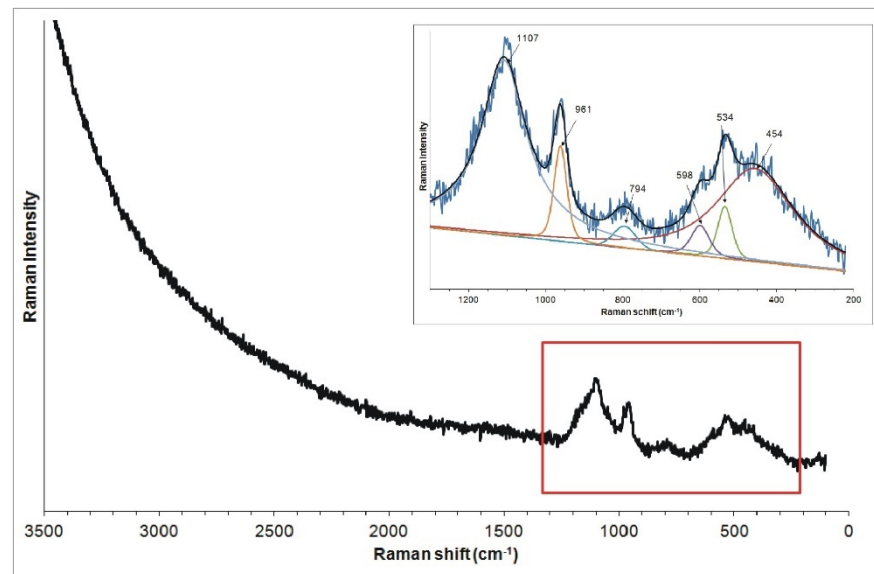


**Figure 8.** Representative characteristic Raman spectrum of the surface of the blue bead.

The Raman investigations of the white substance filling the decorative carving of the bead were hindered by the strong fluorescence of the samples induced by a laser beam. Also, no Raman spectra were recorded that would allow for the identification of the glass corrosion products.

The XRD diffraction pattern of the blue bead surface with the ornament (frontal surface) (Figure 9a) revealed the presence of the following phases: lead chloride hydroxide  $\text{Pb}(\text{OH})\text{Cl}$  (ICDD card no. 52-289) and glass devitrification products, mainly lead silicates (ICDD card no.: 44-271, 31-692, 44-273, 32-514), calcium silicate  $\text{Ca}_2\text{SiO}_4$  (ICDD card no. 23-1042) and an amorphous phase. Furthermore, the presence of calcium phosphate  $\text{Ca}_3(\text{PO}_4)_2$  (ICDD card no. 9-348) is also possible, whereas on its back surface (Figure 9b), quartz (ICDD card no. 33-1161), calcium silicate  $\text{Ca}_2\text{SiO}_4$  (ICDD card no. 23-1042), lead silicates (ICDD card no.: 44-273, 44-271) and a significant amount of amorphous phase were identified.

### 3.3. The Black Bead from Opening No. 3A

Both sides of the bead (the top and bottom) were examined.

Representative SEM-EDS analysis results are shown in Figure 10 and Table 4 and results of Raman microspectroscopy analysis, in Figure 11.

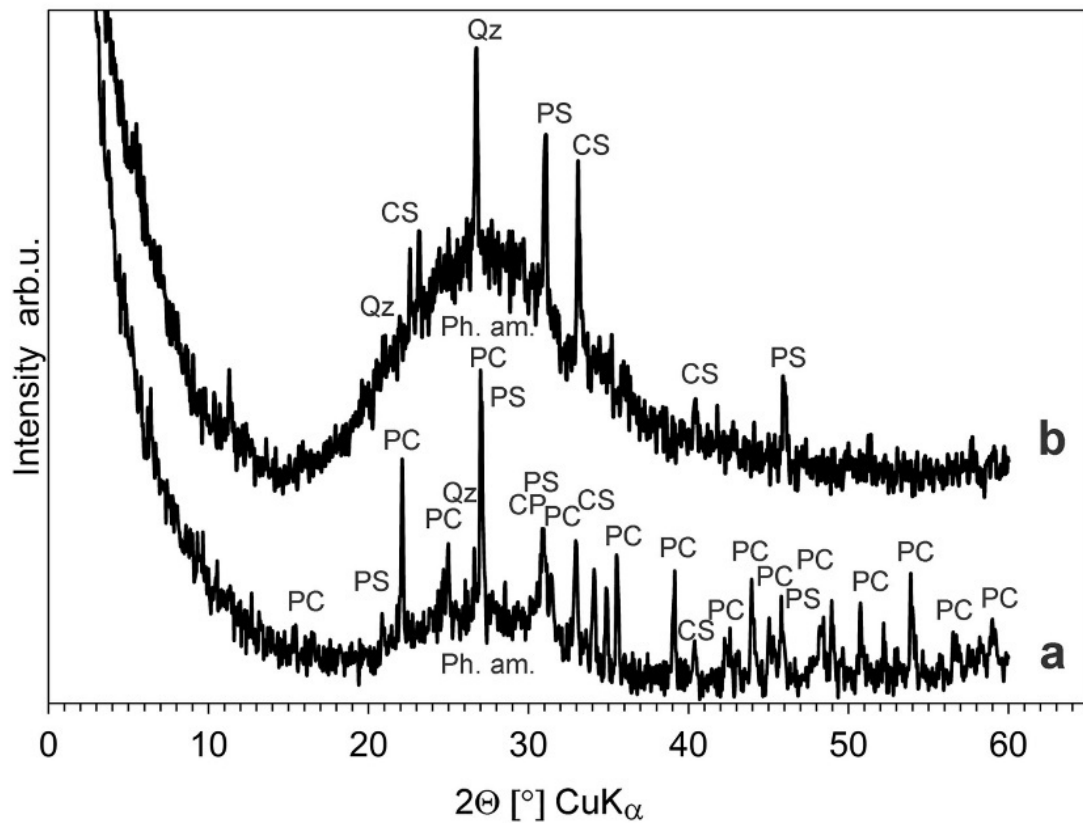


**Figure 9.** Characteristic X-ray diffractogram of the blue bead: (a) surface with a white substance filling the bead ornamentation, (b) the underside surface of the bead. Abbreviations: PC— $\text{Pb}(\text{OH})\text{Cl}$  (52-289), PS— $\text{Pb}_{36}((\text{Si}_2\text{O}_7)_6(\text{Si}_4\text{O}_{13})_3\text{O}_3)$  (44-271),  $\text{Pb}_{33}(\text{Si}_2\text{O}_7)_6(\text{Si}_4\text{O}_{13})_3$  (44-273),  $\text{Pb}_5\text{Si}_3\text{O}_{11}$  (31-692), PCS— $\text{Pb}_8\text{Ca}(\text{Si}_2\text{O}_7)_3$  (32-514), CS— $\text{Ca}_2\text{SiO}_4$  (23-1042), Qz—quartz  $\text{SiO}_2$  (33-1161), CP— $\text{Ca}_3(\text{PO}_4)_2$  (9-348), Ph. am.—amorphous phase.

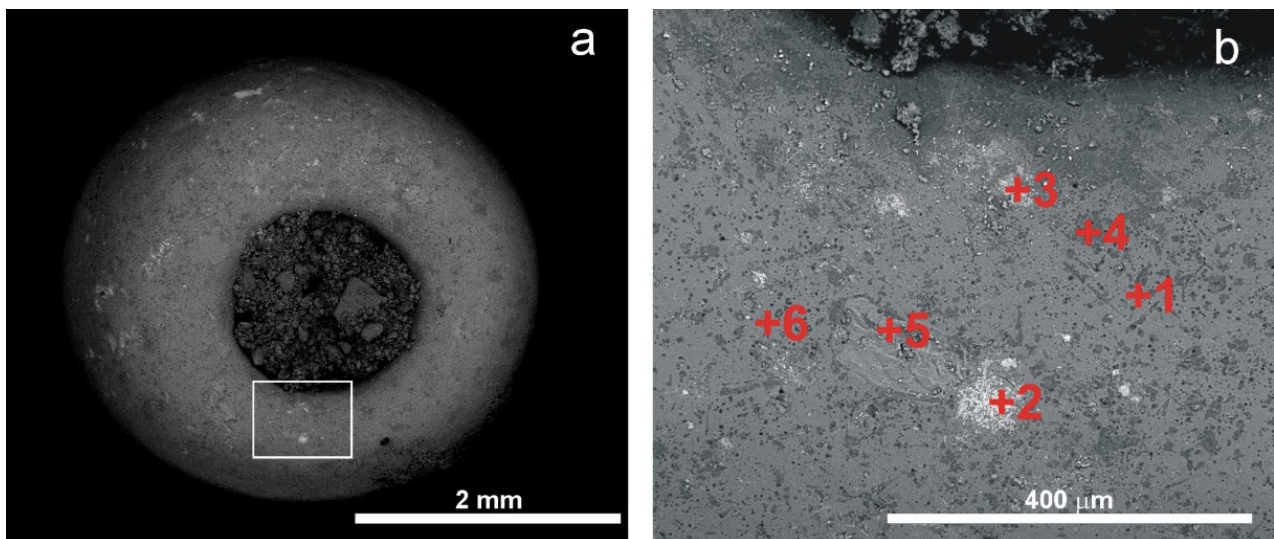


**Figure 10.** Backscattered electron (BSE) image of the surface of the black bead (a,b). For chemical analyses obtained at the points numbered 1–6, see Table 4.

**Table 4.** Chemical composition, in weight percentage, of the black bead. For all elements (except anion Cl), the composition is expressed as oxides weight %. The exact positions of the analysed points are shown in Figure 10.

	Analysed Points					
	+1	+2	+3	+4	+5	+6
CO <sub>2</sub>	b.d.l.	12.40	10.40	b.d.l.	b.d.l.	b.d.l.
N <sub>2</sub> O <sub>5</sub>	b.d.l.	b.d.l.	b.d.l.	b.d.l.	b.d.l.	b.d.l.
Na <sub>2</sub> O	12.25	2.70	3.46	4.48	10.48	11.09
MgO	3.39	1.02	1.01	1.13	3.11	3.36
Al <sub>2</sub> O <sub>3</sub>	3.02	2.94	2.88	4.10	3.35	2.85
SiO <sub>2</sub>	63.20	38.35	46.03	77.57	61.59	62.47
P <sub>2</sub> O <sub>5</sub>	0.58	7.22	6.23	0.44	0.63	0.81
SO <sub>3</sub>	0.41	0.42	0.35	0.42	0.47	0.46
PbO <sub>2</sub>	2.09	18.14	14.83	0.83	2.38	2.01
Cl	0.81	2.18	2.34	1.45	1.05	0.81
K <sub>2</sub> O	2.32	1.14	1.12	1.69	2.20	3.66
CaO	6.09	9.46	7.69	3.68	7.87	5.74
MnO	3.85	1.14	1.03	1.10	5.15	3.84
Fe <sub>2</sub> O <sub>3</sub>	1.13	1.87	1.57	2.10	1.72	1.48
CoO	0.20	b.d.l.	0.18	0.11	b.d.l.	0.34
NiO	0.15	0.28	0.27	0.22	b.d.l.	0.17
CuO	0.31	0.40	0.36	0.27	b.d.l.	0.35
ZnO	0.20	0.32	0.27	0.41	b.d.l.	0.55
Total	100.00	100.00	100.00	100.00	100.00	100.00

b.d.l.—below detection limit.

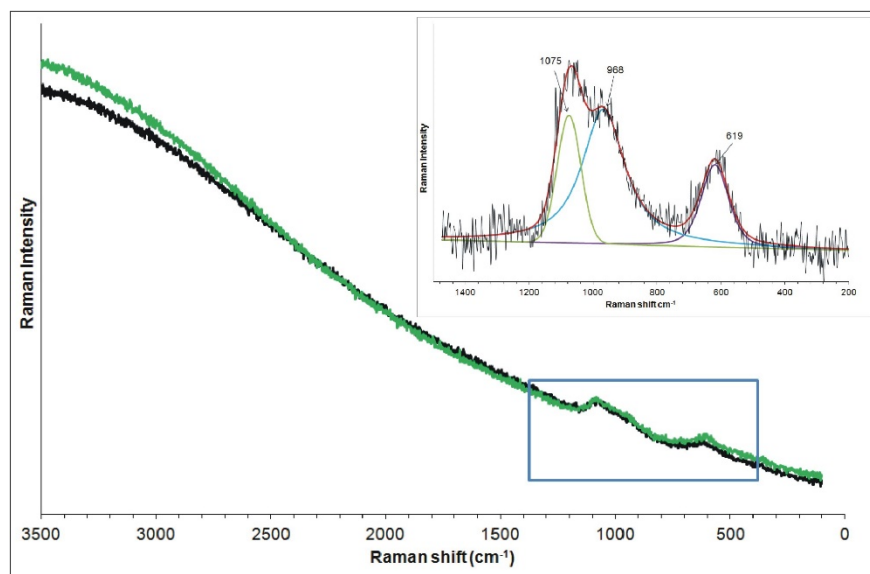


**Figure 11.** Representative characteristic Raman spectra of the surface of the black bead.

EDS chemical analysis of the bead surface (Figure 10, Table 4, points 1, 5 and 6) mainly showed the presence of Si (mean SiO<sub>2</sub>: 66.21 ± 6.56 wt%), Na (mean Na<sub>2</sub>O: 9.58 ± 3.01 wt%), Ca (mean CaO: 5.85 ± 1.49 wt%), K (mean K<sub>2</sub>O: 2.47 ± 0.73 wt%), Mg (mean MgO: 2.75 ± 0.94 wt%) and Al (mean Al<sub>2</sub>O<sub>3</sub>: 3.33 ± 0.48 wt%). In addition, the presence of Pb (mean PbO<sub>2</sub>: 1.83 ± 0.59 wt%), Mn (mean MnO: 3.49 ± 1.42 wt%) and Fe (mean Fe<sub>2</sub>O<sub>3</sub>: 1.61 ± 0.35 wt%) was recorded. The presence of Co, Ni, Cu and Zn was also detected in all analysed points. Their concentrations did not exceed 0.55 wt%.

In some places on the surface of the bead, fine-grained accumulations were observed (Figure 10, Table 4, points 2 and 3). At these points, EDS analysis shows the presence of Pb (mean PbO<sub>2</sub> 16.48 ± 1.65 wt%), the other constituents being Si, Na, Ca, K, Mg, Mn,

Fe, Al and P. These elements were also recorded in analyses of the surface areas which did not show such granular accumulations. C, Cl and S are most likely associated with corrosion products. The results from measuring point 4 probably reveal the presence of a gel layer and the constituent elements of the glass. The glass is locally enriched in SiO<sub>2</sub> due to the leaching of metal elements and alkaline earth metals (dealkalization), indicating local corrosion of the glass surface; perhaps it was the effect of small, local heterogeneities in the glass.

The Raman spectrum shows two very weak broad bands in the range of 450–1150 cm<sup>-1</sup> (Figure 11), suggesting the amorphous nature of the substance. After baseline correction, the spectrum consists of a band in the range of ~450–700 cm<sup>-1</sup> with the maximum at 619 cm<sup>-1</sup> and a band in the range of 800–1150 cm<sup>-1</sup> with two peaks at 968 and 1075 cm<sup>-1</sup>. Bands at 619 cm<sup>-1</sup> and 1075 cm<sup>-1</sup> probably represent Si–O bending and stretching vibrations, respectively [20,25]. The band at 968 cm<sup>-1</sup> can be ascribed to the presence of phosphate (PO<sub>4</sub><sup>3-</sup>) groups. As in the case of the blue bead, the Raman spectrum obtained suggests that the analysed material is glass.

Due to the strong fluorescence of the samples induced by the laser beam, no Raman spectra allowing the identification of the glass corrosion products were recorded. The black bead X-ray pattern obtained from a non-flat surface of the bead (for the XRD technique, a flat surface is required; due to the shape and size of the bead this technique was not available, as stated in 'Materials and Methods') was almost identical to the cross X-ray pattern and did not allow any meaningful interpretation.

## 4. Discussion

### 4.1. The Cross

On the basis of analysis, the cross was found to be made of rock crystal. Rock crystal is a colourless and transparent monocrystal belonging to the group of automorphic quartz. Due to its purity, high hardness and resistance to chemical postdepositional processes, including weathering, quartz is a valuable material used by man since prehistoric times. Determining the origin of the rock crystal from which the object was made is quite difficult. Admittedly, the analysis of inclusions incorporated during the growth of the crystal, using Raman microspectroscopy, could answer this question; however, it requires a database of inclusion characteristics of particular gemstone deposits in the world. In the absence of such a database, they can only be based on simultaneous comparative analyses of both inclusions in objects and raw materials from probable sourcing sites [26]. Moreover, Raman studies are sometimes hampered by the strong fluorescence of the samples caused by the laser beam, making the analysis unreliable. Such extensive research, however, is beyond the scope of this paper.

The cross is probably framed with an alloy of gold, silver and copper; we did not observe signs that would suggest the use of gold leaves to cover the silver–copper alloy. However, the approximated chemical composition of the metal frame can only be obtained by cross-section analysis, not available during the study.

### 4.2. The Beads

In the case of the beads, the recorded Raman spectra suggested the presence of an amorphous or very poorly crystalline substance, in which characteristic bands of glass were identified [20,24,25]. To corroborate our findings, the identification of the beads' composition had to be crosschecked using Raman microspectroscopy, SEM-EDS results and XRD.

#### 4.2.1. Chemical Composition of the Beads

The SEM-EDS method is a surface-sensitive technique with an analysis depth of about a few µm, depending on the absorption coefficient of the materials [27]. The chemical composition determined characterizes the surface of the bead subjected to several centuries of influence from the environment in which it was found. Due to the necessity of using

non-destructive and non-invasive techniques, the composition of the interior, unaltered part of the bead could not be established. It was therefore uncertain whether elements such as Pb and other heavy metals, but also elements occurring in quantities of a few %, such as K, Ca, Na and others, are components of the manufacturing material alone, or whether they originate from the environment (as a contaminant). However, although the cross and the beads were found in different locations (different risers), the accompanying elements are very similar (they are: soil and gravel, conifer needles, textiles, paper, corroded reliquary fragments and wax seal). Therefore, they do not appear to have caused any changes in the chemical composition of the artefacts studied. This is suggested by the chemical composition of the cross material, which is exclusively Si and O. Thus, the complete absence of other chemical elements in the case of the cross supports the idea that, in the case of the beads, they are components of the material from which the beads were made. Besides Si, K, Na and Ca, the presence of lead (mean  $\text{PbO}_2$ : 2 wt%) seems to be the most significant. If it does not come from the environment and is a component of the bead material, it suggests that the bead is made from alkaline glass containing Pb (probably to improve its properties and also to modify other colours) [28].

Although glass technology has changed through time, glass is usually made of a few main components: glass formers or vitrifiers, fluxing agents or glass modifiers, glass stabilizers and also opacifiers and glass colouring/or decolouring agents. Silica (either in the form of sand or coarse quartz pebbles) is the most common glass former. The fluxing agent, typically an alkaline oxide (sodium-, potassium- or lead-rich compounds; e.g., an evaporitic deposit raw material or plant ashes), was used to lower the melting temperature. To make the mixture more stable and resistant to deterioration, calcium- or aluminium-based compounds were added [28–30]. The use of different raw material sources and distinct glass recipes causes the composition of glass to change according to its provenance. [28,31]. Different components, colourants and opacifiers (such as metallic oxides, salts, lead, phosphorus and antimony compounds) were also added to modify the physical properties of the glass. Because all of these components frequently contain some impurities, they may reflect their origin or the manufacturing processes. Nevertheless, analyses of these impurities often require the use of more invasive techniques with lower detection limits than SEM-EDS, such as XRF with an analysis depth of a few microns to a few millimetres (depending on absorption coefficient) [32]. However, because the glass was also recycled, such interpretation of data sometimes needs to be more complex [28,33].

The chemical composition of the beads studied was initially used to classify the beads according to glass type, as either soda-rich, potash-rich or mixed alkali glass. The ternary diagram of the normalized concentrations of  $\text{Na}_2\text{O}$ ,  $\text{K}_2\text{O} + \text{MgO}$  content (indicative for plant ash glass) and CaO has allowed us to define the main chemical glass types based on their alkali metal source [28,34,35]. The classification of the blue bead is not obvious. Figure 12 shows that the blue glass beads belong to both the compositional window of sodium–potassium mixed alkaline glass—group III and group IV—forest plant-ash potash–lime glass (the projection points are on the border of both composition groups, i.e., III and IV). However, since this glass contains a much higher amount of potassium than sodium (mean:  $\text{K}_2\text{O}$  11.26 wt%,  $\text{Na}_2\text{O}$  2.50 wt%, CaO 6.32 wt%), magnesium ( $\text{MgO}$ : up to 1.06 wt%; mean 0.75 wt%), and considering that potassium and magnesium are typical of plant ash glasses, this glass seems more likely to be classified as forest plant-ash potash–lime glass. The presence of phosphorus (mean  $\text{P}_2\text{O}_5$ : 2.33 wt%), might also be connected to the ash, although also to the opacifying agents. The black bead belongs to the soda–lime plant ash glass (group II) (mean:  $\text{K}_2\text{O}$  2.47 wt%,  $\text{Na}_2\text{O}$  9.58 wt%, CaO 5.85 wt%), where calcium and sodium were added in the form of plant ashes rich in these elements (most likely halophytic plants incinerated in order to produce soda ash). As technology improved, plant ash was replaced by industrial chemicals, resulting in soda–lime glasses where magnesium and potassium, typical of plant ash glass, are absent [25,35].

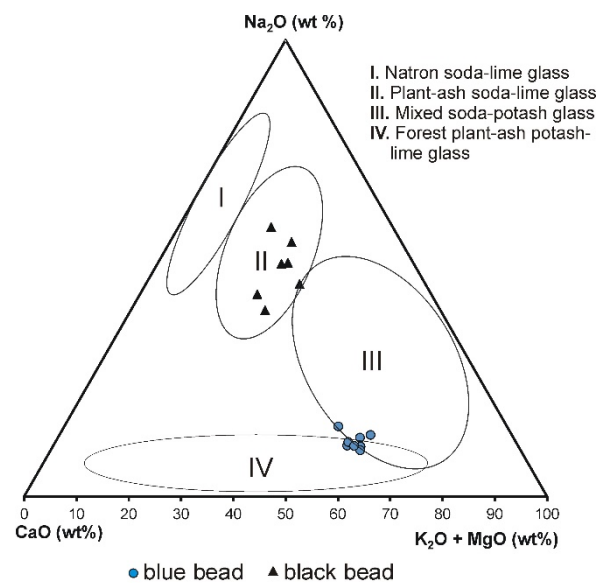


**Figure 12.** Ternary diagram of the normalized  $\text{Na}_2\text{O}$ ,  $\text{K}_2\text{O} + \text{MgO}$  and  $\text{CaO}$  contents of the two glass beads analysed by EDS. Four main chemical glass types are evidenced by the ellipses [28].

The identification of the glass type based on the measurement of the two main Raman bands wavenumber maxima (bending and stretching modes of the  $\text{SiO}_4$  tetrahedron respectively) [20,33,36] confirm that the black bead is a soda–lime glass type (619 and  $1075\text{ cm}^{-1}$  maxima of bending and stretching modes, respectively; see Figure 11) and the blue bead is a high-potassium, potash–lime glass type ( $534$  and  $1107\text{ cm}^{-1}$  maxima of bending and stretching modes, respectively; see Figure 8).

The glass of the blue and black bead clearly differs in their  $\text{Na}_2\text{O}$  and  $\text{K}_2\text{O}$  content (Figure 13); the blue bead shows higher a concentration of potassium oxide than the black bead and represents potash glass (mean  $\text{K}_2\text{O}$ : 11.26 wt% and 2.47 wt%, respectively), whereas the black bead contains a higher concentration of sodium oxide and represents soda–lime glass (mean  $\text{Na}_2\text{O}$ : 9.58 wt% and 2.50 wt%, respectively).

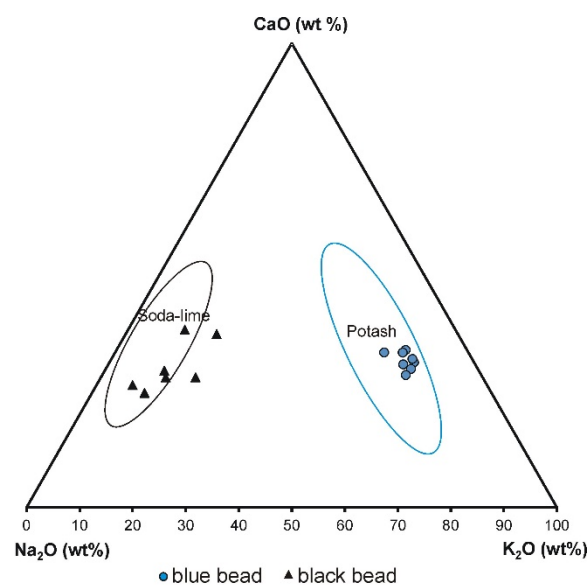


**Figure 13.** Variety of the glass flux compositions depicted in the  $\text{Na}_2\text{O}$ – $\text{K}_2\text{O}$ – $\text{CaO}$  ratio [20].

A diagram plotting the aluminium oxide content, magnesium and potassium oxides content (typical of plant ash glasses) and calcium oxide content against each other shows

that both blue and black beads represent low alumina glass plant ash. (Figure 14). This may suggest that the glass originated in northern or central Europe or Venice, as generally, these glasses contain less alumina (usually less than 3%) when compared to southern European glass (except Venetian) [20]. The differences in potassium, magnesium and phosphorus content in the two beads are also clearly seen in Figure 15a,b. The glass of the blue bead is enriched in potassium and phosphorus, while the black bead contains more magnesium.

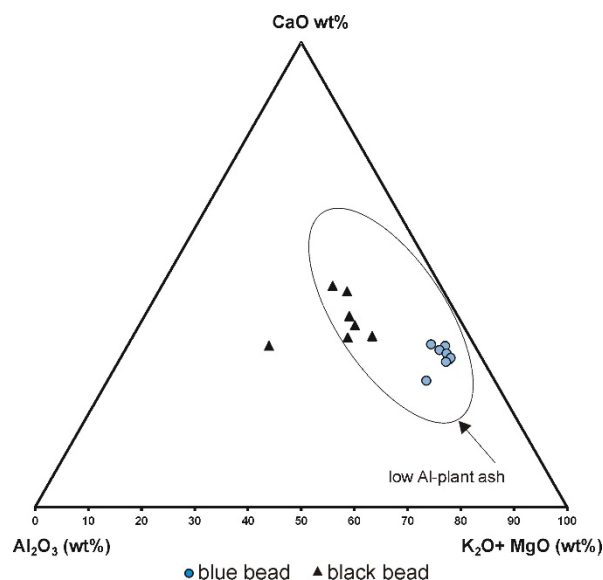


**Figure 14.**  $\text{Al}_2\text{O}_3$ – $\text{CaO}$ – $\text{K}_2\text{O}+\text{MgO}$  ratio diagram [20] of the two glass beads analysed by EDS.

#### 4.2.2. Chemical Composition Versus Possible Provenance and Chronology of the Beads

The chemical composition of the glass is influenced by the composition of raw materials from different regions and the specific recipes of glass production. Alumina may have been introduced into the glass not only as glass stabilizers but also through the use of poorly refined sand [37]. The composition of the ash (used as the fluxing agent) depends on the plant type and plant habitat [20,28,38] and can have large chemical variations, even for a single plant species [38]. Ashes contain variable amounts of quartz  $\text{SiO}_2$ , calcite  $\text{CaCO}_3$ , potash  $\text{K}_2\text{CO}_3$ , arcanite  $\text{K}_2\text{SO}_4$ , fairchildite  $\text{K}_2\text{Ca}(\text{CO}_3)_2$ , apatite  $\text{Ca}_5(\text{PO}_4)_3(\text{Cl}/\text{F}/\text{OH})$  and periclase  $\text{MgO}$  and other, also sodic phases [20,34,35]. Thus, elements derived from minerals present in ashes may be present in the glass. Consequently, potassium, magnesium and phosphorus levels in glass began to be higher after the 8th century AD, when potash from plant ash replaced natron (mineral soda obtained from inland lakes) as the main alkaline flux. Ashes from different plants predominated in different parts of Europe. In Western and Central Europe, continental plant ashes rich in potassium were used to produce so-called ‘forest’ glass. In England, algal ash (kelp ash) was used instead of natron, whilst in the Mediterranean region, ash from halophytic plants was employed. Later, plant ashes were replaced by soda ashes imported mainly from Spain (or from other places, such as Sicily, southern France and North Africa); however, the use of potash-rich fluxes continued till the 19th century AD. At the end of the 18th century, industrial soda was also in use (first produced by the ‘Leblanc’ method and after 1861, by the Solvay process) [20,28]; glass manufactured using such new raw materials is characterized by its high sodium content and low levels of contaminants. The beads analysed could therefore have been manufactured after the eighth century and at the latest 1733, when the Chapel of the Scala Santa (Holy Stairs) was consecrated; however, based on available documents, some artefacts may have been added after this date, so the beads may have been made even later.

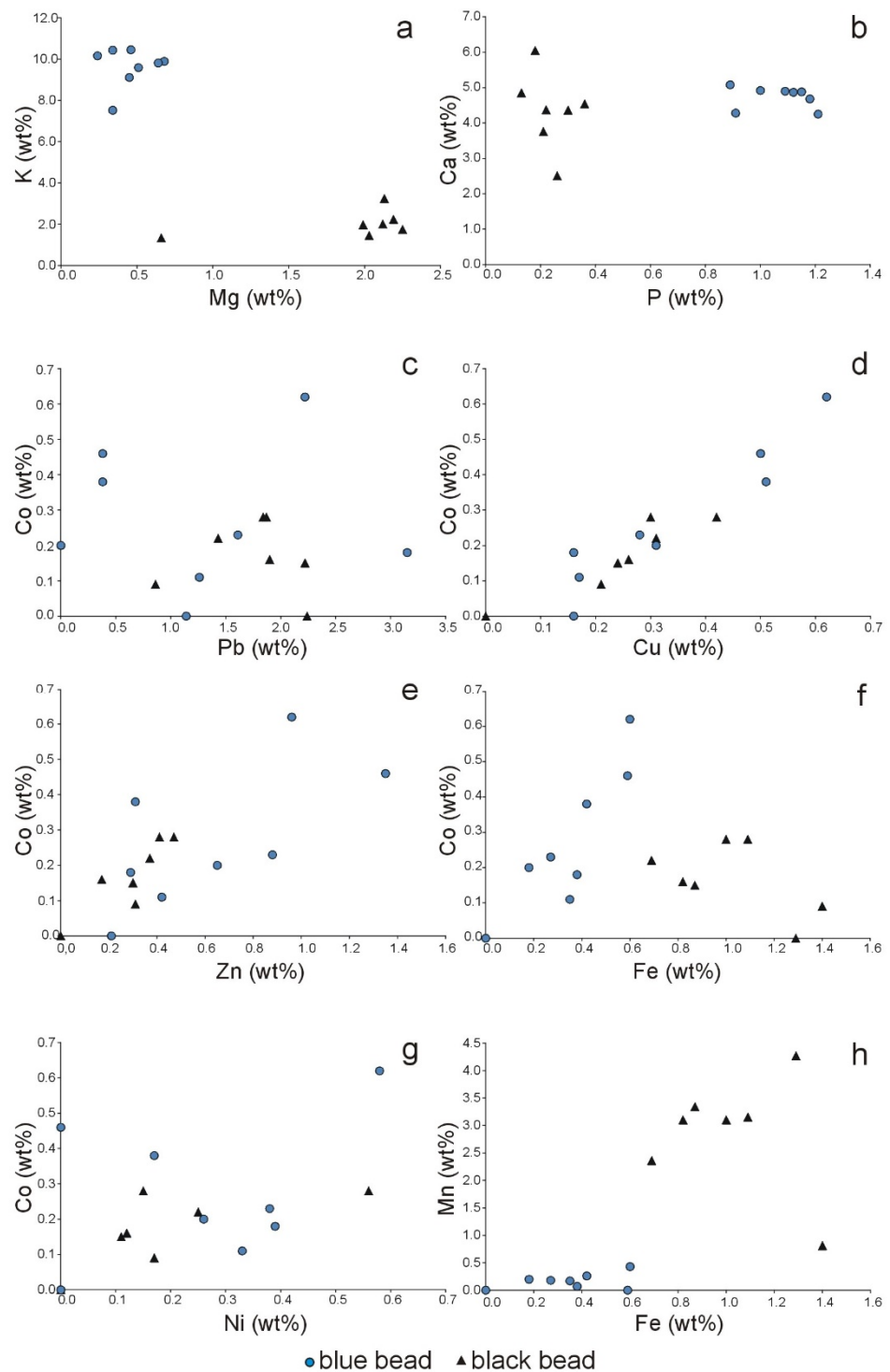


**Figure 15.** Associations between some of the elements detected by EDS in the analysed beads (a–h).

The results obtained from the analysis of the chemical composition of glass may also have been affected by changes occurring on the glass surface over time due to corrosion processes. During the early stages of corrosion, the glass surface is characterized by the arising of a leached layer, depleted of cations. Finally, the formation of crystalline weathering products, mainly sulphates, carbonates and, more rarely, nitrates, chlorides and some organic compounds was observed [39,40]. Therefore, the presence of carbon, chlorine and possibly phosphorus in the beads analysed can be associated with corrosion products of glass; these elements coming from the environment form compounds with

cations leached from glass. However, as mentioned above, they also come from natural resources (e.g., potash  $K_2CO_3$  obtained from plant ash, soda obtained from rock salt or bone meal used as an opacifier), which may have been used in glass production [39]. The possible presence of calcium phosphate has been confirmed by Raman microspectroscopy. The strong band at  $961\text{ cm}^{-1}$ , present in the spectrum of the blue bead (Figure 8), may be related to calcium phosphate, probably used as opacifiers [20,24]. A similar, but broader band was observed in the Raman spectrum of the black bead (Figure 11). Chemical analyses by EDS confirmed the presence of calcium and phosphorus in both beads, but the blue bead is more enriched in P than the black one (mean  $P_2O_5$ : 2.33 and 0.61 wt%, respectively; see Figure 15b). XRD analysis of the blue bead also suggested  $Ca_3(PO_4)_2$  as a possible phase. Calcium phosphate, generally introduced in the form of burnt bones, has been used as an opacifier since the fifth century CE and is commonly mentioned in Venetian recipe books since the 14th century CE [31]. Differing phosphorus levels for the blue and black bead analysed may also reflect the different types of plants used to produce the ash [38].

Another element that attracts attention is lead. Pb is particularly important in glass production since it can act as a glass former and modifier, but it can also influence both transparency and colour [30,39,41,42]. Lead was observed at similar levels (about 2 wt% of  $PbO_2$ ) in both beads (Figure 15c), which may also suggest its intentional addition to improve the properties of the glass. The concentration of lead compounds in the blue bead's ornamentation, also observed in other places on the surface of both the blue and black bead (Figures 6, 7 and 10), may indicate that these are corrosion products of glass containing Pb. The XRD diffraction pattern of the blue bead revealed the possible presence of various lead phases being products of glass devitrification and weathering (lead silicates and lead chloride hydroxide,  $Pb(OH)Cl$ ). The presence of lead in trace amounts is found in many medieval glasses. This group includes late medieval glass from so-called 'forest glasshouses' [39]. However, when it comes to the blue bead, lead compounds could also have been introduced intentionally to emphasize the sculptural ornament on its surface, forming a kind of inlay. Therefore, this hypothesis cannot be ruled out either.

#### 4.2.3. Colour of the Beads

The chemical composition of the blue bead discovered in Scala Santa seems to explain its colour. For that particular bead, cobalt was found in small amounts, and its concentration is less than 1 wt% (mean CoO: 0.33 wt%) (Tables 2 and 3). However,  $Co^{2+}$  ions are among the most common colouring agents present in ancient glass [31]. Even at low concentrations, due to their high absorption coefficient, cobalt ions produce a distinct blue colour. According to Dussubieux and Gratuze [43], the strongly blue-stained beads were found to contain CoO at very low levels of 0.07–0.3%. Considering the low concentrations that these results show, it remains below the detection limit for quantification using the EDS method and may explain the absence of Co peaks in some of the recorded spectra (EDS detection limit is 0.02 to 0.1 wt% and varies depending on the atomic number of the element) [44]. In addition, the co-occurrence of copper, zinc and iron with cobalt was observed. (Figure 15d–f). Moreover, a linear increase in the concentration of each of these elements (Cu, Zn and Fe) is also observed with increasing cobalt concentration. The simultaneous presence of cobalt and copper can result in a light blue hue to the bead [31]. Nickel is also present, but its concentration does not show a clear trend (Figure 15g). These elements may have been added to the glass along with the cobalt colourant, possibly also containing lead.

Generally, the blue colour of the glasses may be related to  $Co^{2+}$  ions, cobalt silicate/aluminate, cobalt oxide or spinel, sulphur in lapis lazuli grains  $(Na,Ca)_8(Al_6Si_6O_{24})(S O_4,Cl,S)_2$  and copper in cuprorivaite  $CaCuSi_4O_{10}$ —Egyptian blue and its Chinese barium homologue [20,45]. Until the 19th century, the source of cobalt was mainly natural ores containing large amounts of other transition metals such as manganese, iron, arsenate, chromium and others [46,47]. These minor and trace element associations may indicate the source of the pigment and could be the fingerprint of the glass [28,42,48]. In the research

presented, the elemental association of Co–Cu–Zn–Fe–Ni was observed, although it is possible (although it is unclear) that lead should also be included here. However, other metals such as arsenic and other elements listed by Gratuze [28] may also be present. However, their concentration may be below the detection limit of the EDS method. The presence of copper is also problematic; we cannot state conclusively that the copper was not added intentionally, e.g., to change the shade of blue. Cobalt is often combined with other colouring agents, which have various effects on the shade of the glass. This also includes elements derived from ore (e.g., Mn, Cu, Fe or Ni), that can influence the colour, depending on the furnace atmosphere [39,42]. therefore, we cannot state definitively the source of the pigment used.

In the case of the black beads, enrichment in Mn and Fe and a clear correlation between these elements is observed (Figure 15h). Manganese oxide concentrations vary from 1.10 to 5.15 wt% (mean MnO: 3.48 wt%) and iron oxide from 1.13 to 1.72 wt% (mean Fe<sub>2</sub>O<sub>3</sub>: 1.61 wt%). The glass also contains small amounts of zinc (mean ZnO: 0.29 wt%) copper (mean CuO: 0.23 wt%) and cobalt (mean CoO: 0.16 wt%) (Table 4). Their concentration is lower than that of the blue bead. The raw materials introducing manganese may have been various manganese compounds oxides, hydroxides or spinels [47,49,50]. Among Mn-spinels, jacobite (Mn<sup>2+</sup>, Fe<sup>2+</sup>, Mg) (Fe<sup>3+</sup>, Mn<sup>3+</sup>)<sub>2</sub>O<sub>4</sub> is an important ore mineral, which is simultaneously a source of iron. Admixtures of Mg, Al and Zn are also characteristic of jacobite [49]. It is possible that the higher Mg content (mean MgO 2.75 wt%) is the result of using jacobite as a pigment (magnesium is a common admixture in Mn and Fe compounds [51]). However, magnesium may also come from the ash used as the flux.

#### 4.3. Historical and Cultural Context

In a historical and cultural context, according to tradition, the reliquary cross contains a particle of the True Cross. The Lignum Vitae with the remaining Instruments of the Passion formed the group of the most precious relics in Christianity already in late antiquity [52–54]. The acquisition of a minute sliver increased the importance of a sanctuary that also became a destination for crowds of the faithful and pilgrims [55]. This cross form was manufactured in series. Reliquary crosses made from rock crystal were produced following a single pattern, freely transformed as required. Modifications were introduced principally to the form of an ornament that was always made using the filigree technique but with varying decorative values. A cross similar to that discovered in the Piarist church was exhibited in St. Nicholas collegiate church in Końskie (Poland), where a document confirming its authenticity was found in March 2016. The contents of the document demonstrate that reliquaries of this type were handed over to pilgrims already in Rome ( . . . *we placed it in a crystal cross . . .* ) with particles of the True Cross inside, bound using thread and sealed. The relic was frequently put into an additional more or less decorative package, with the sealed crystal reliquary preserved untouched. In the church of the Cracow Piarists, this additional “package” was offered by the monumental Holy Stairs. This form of reliquary cross was popular throughout Europe [56,57]. Transparent reliquaries gained in popularity from the early 13th century. This trend was consistent with the guidelines set out by the Fourth Lateran Council held in 1215, recommending that relics revered by the faithful be not only authenticated but also visible while being effectively protected. A new type of reliquary appeared known as an ostensorium (Latin ‘ostendere’ means ‘exhibit’) [58,59].

An analysis of available preserved documents confirming the authenticity of relics contained in similar crosses (made from rock crystal) indicates their popularity from the turn of the 17th and 18th centuries (with its peak in the early 18th century) to the early 19th century. Crosses with fragments of the True Cross were brought from Italy. An intensified pilgrimage movement promoted a replicable form of encasement designed exclusively for particles of the True Cross.

The topic of beads is more complex and debatable. The blue and the black bead might belong to the class of non-significant relics (objects that have come in direct contact with a saint or blessed) or were brought to Cracow as souvenirs from the Holy Land. The absence

of official documents confirming those facts hinders the dating of the components or the determination of their origin or relation to a specific saint. The blue bead represents a mysterious object. Its identification is difficult due to the absence of a hole. Certainly, it was a decorative element. It could serve as a fragment of ceremonial dress, jewellery or vessel. It could belong both to the sacred and the profane sphere. The black bead is less mysterious; it could be a rosary bead. Their glass material may indicate their Italian origins. Venetian glass played a particularly important role in the European market. Venetian glass beads, buttons and various types of jewellery, such as rings, earrings, bracelets and crosses, enjoyed huge popularity. Glass beads were colourless, “crystal” or coloured. Rosaries were also made from glass beads [60]. However, considering mediaeval tradition, a non-practical function for the beads cannot be ruled out. These items could have had a symbolic or even magical meaning. Single glass beads put into graves could have played the role that amulets did in the Middle Ages [41,61].

## 5. Conclusions

This study contains findings on three particularly interesting objects discovered in the Scala Santa (Holy Stairs) located in the crypt under the Piarist Church in Cracow (Poland), which was originally designed as a chapel of the Holy Stairs, a unique historical object in world terms. They are: a metal, framed, transparent reliquary cross containing a particle of the True Cross and two opaque beads—a decorated, undrilled blue bead and a drilled black bead. In spite of the limitations resulting from the necessity to use only non-invasive and non-destructive methods (scanning electron microscopy with energy dispersive spectrometry (SEM–EDS), Raman microspectroscopy (RS) and X-ray diffractometry (XRPD)) to study the chemical composition and structure of these artefacts, the research carried out provided a great deal of information on the material from which the objects found in the Holy Stairs were made. The inability to determine the bulk composition of the glasses makes it impossible to precisely determine the possible site of bead manufacture. However, the presented material characterization of the artefacts, despite its imperfections (the research limited to some specific methods) allows a discussion of these issues, extends the knowledge of the objects placed in the Holy Stairs and considers them worthy of being placed there.

The transparent reliquary cross containing a particle of the True Cross was found to be made of rock crystal and framed with an alloy of gold, silver and copper. Considering the popularity of reliquary crosses made from rock crystal at the turn of the 17th and 18th centuries, the Piarist object may be dated to the beginnings of the use of the Holy Stairs chapel that was consecrated in 1733.

Analyses indicate that the beads are made of glass. Considering the source of the flux, the glass can be divided into two main types: forest plant-ash potash–lime glass (the blue bead) and plant-ash soda–lime glass (the black bead). Thus, the beads were produced after the eighth century (introduction of plant ash as a source of alkaline flux) and at the latest, around 1733, when the chapel of Holy Stairs was consecrated. However, based on available documents, some artefacts may have been added after this date; therefore, the beads may have been made even later. Ash from different plants (of different compositions; potash and soda, respectively) was used to produce the glass. Therefore, this suggests that the glass may have been manufactured in different geographical regions (of Europe). The production of potash–lime glass developed in northern and central European manufacturing centres throughout the Middle Age. Heavily forested areas favoured the use of wood ash as the raw material for glass production (this type of glass is known as ‘forest glass’). It is therefore likely that the blue glass bead was produced in Central Europe. However, even though the Venetian glassmaking industry traditionally used soda plant ash (derived from halophytic plants) as their main glass modifier, potash plant ashes, produced by burning inland plants, were occasionally employed as well. Thus, this site cannot be ruled out as the site of manufacture of the blue bead. The black bead falls under the compositional window of plant-ash soda–lime glass, and the place of its production, in this case, might

have been associated with centres using the ashes of sodium-rich plants as a flux, as was the case, for example, in the Venetian glassmaking industry. This type of plant ash from various regions of the world (first from the Levantine coast, then from Spain and other places) was used there from the 13th century and were commonly employed in the 16th and 17th centuries and later.

Since both of these glass beads are opaque and there is enrichment and association between P and Ca, especially in the case of the blue bead, this suggests that calcium phosphates might have been used as opacifying agents. The characteristic Raman band of phosphate ions was observed in the case of both beads. Although both beads revealed similar calcium levels, the differing levels of phosphorus may also reflect different types of plants used for ash production.

Chemical data indicate that cobalt ions were used to produce the blue hue of the ornamented glass bead. However, the tint might have been further modified by adding Cu, which was also found in the glass. Combining metallic ions such as manganese and iron was used to produce the black hue of the drilled bead. However, it is difficult to pinpoint the exact source of the pigments used due to the lack of data on the presence of some trace elements that may be present below the detection limit of the EDS method. These elements may be characteristic of particular ores, which can help indicate the source of the pigments.

Lead was present in both beads as one of the minor components and was also found as a constituent of the corrosion products (lead silicates and lead chloride hydroxide) on their surfaces. It may have been introduced intentionally to improve the properties of the glass, or it may be a component of the raw materials, e.g., ores, which were employed as pigments. Of special note is the concentration of lead compounds in the blue bead ornamentation. It is possible that the carving favoured the accumulation and retention of the corrosion product, although it cannot be ruled out that the lead compounds were introduced intentionally to emphasize the decoration. Nevertheless, no confirmation of such practices has been discovered in the available literature, so this question has remained open. Lack of official documents confirming the status of non-significant relics (objects in direct contact with a saint or blessed person) or that they were brought to Cracow as souvenirs from the Holy Land hinders the dating of the beads and connection to a specific saint person. Their function cannot be clearly identified. The black bead was probably a rosary bead. The blue bead was purely decorative. However, it cannot be determined whether it was part of a costume, an item of jewellery, or a vessel.

**Author Contributions:** Conceived and designed the experiments: M.M. and A.G. Mineralogical and geochemical analyses (SEM-EDS, RS, XRD): performing, interpretation of results, discussion, conclusions, writing of manuscript, visualization, preparation of figures: M.M. and A.G. The historical section: E.B. Art-history discussion and conclusion: K.P. Art conservation problems, macroscopic observations, the formal description of the objects: K.P. Proofreading: M.M. and K.P. All authors have read and agreed to the published version of the manuscript.

**Funding:** The studies were supported by the AGH University of Science and Technology, Kraków, grant number 16.16.140.315.

**Acknowledgments:** We would like to thank Paweł Romanowicz, the author of the photographs and their graphic layouts (Figures 1–3).

**Conflicts of Interest:** The authors declare no conflict of interest.

## References

1. Bochnak, A.; Samek, J. *Katalog Zabytków Sztuki w Polsce, Miasto Kraków, Kościoły i klasztory Śródmieścia, Volume IV, Part III*; Instytut Sztuki Polskiej Akademii Nauk: Warszawa, Poland, 1978; pp. 95–108.
2. Hryszko, B. Zeuxis Moravici Przyczynek do badań nad twórczością Franciszka Ecksteina na Śląsku Opawskim, w Krakowie i we Lwowie. In *Między Wrocławiem a Lwowem, Sztuka na Śląsku, w Małopolsce i na Rusi Koronnej w czasach nowożytnych*; Betlej, A., Brzezina-Scheuerer, K., Oszczanowski, P., Eds.; Acta Universitatis Wratislaviensis: Wrocław, Poland, 2011; pp. 341–347.
3. Rożek, M. *Przewodnik po Zabytkach i Kulturze Krakowa*; Państwowe Wydawnictwo Naukowe: Warszawa, Poland; Kraków, Poland, 1993; pp. 95–96.

4. Buszko, E. Historia kościoła i klasztoru oo. pijarów ze szczególnym uwzględnieniem krypty i zachodniego skrzydła konwentu. In *Dokumentacja Historyczno-Badawcza prac Przeprowadzonych w Latach 2017–2019 w Obrębie Kolegium i Dolnego Kościoła*; (Firma Konserwatorska Piotr Biało Zabytki Malarstwa, Rzeźby, Architektury Sp. z o. o.); Zbiory Archiwum Wojewódzkiego Urzędu Ochrony Zabytków Krakowa: Kraków, Poland, 2020; p. 128.
5. Szmerek, A. Dziewiętnastowieczne inwentarze majątkowe jako źródło do poznania dziejów krypty w kościele Przemienienia Pańskiego oo. Pijarów w Krakowie. *Archiva* **2018**, *11*, 99–116.
6. Koziana-Biało, H.; Pachuta, K. *Dokumentacja Powykonawcza Prac Przeprowadzonych w Latach 2017–2020, Prace Konserwatorskie Przy Wybranych Elementach Wystroju i Wyposażenia Dolnego Kościoła, Zespół Klasztorny OO. Pijarów przy ul. Pijarskiej 2 w Krakowie*; (Firma Konserwatorska Piotr Biało Zabytki Malarstwa, Rzeźby, Architektury Sp. z o. o.); No.: 77942-77943; Zbiory Archiwum Wojewódzkiego Urzędu Ochrony Zabytków Krakowa: Kraków, Poland, 2021; Volume 2–3, p. 456.
7. Horsch, N. *Ad Astra Gradus, Scala Sancta und Sancta Sanctorum in Rom unter Sixtus V (1585–1590)*; Hirmer Verlag: München, Germany, 2014; p. 368.
8. Wyczawski, H.E. *Kalwaria Zebrzydowska, Historia Klasztoru Bernardynów i Kalwaryjskich Drózek*; Calvarianum: Kalwaria Zebrzydowska, Poland, 2006; p. 526.
9. Kogut, M. *Święte Schody w Sośnicy*; Antykwa: Wrocław, Poland, 2010; p. 27.
10. *Resignatio Rectoratus Domus Cracoviensis Facta per Patrem Stephanum a S[anct]o Adalberto Finitis Annis Duodecim sui Officii in Manus R. Patris Bernardi a S. Antonio Rectoris Designati Anno Domini 1733 die 1ma Mensis Octobris*; No.: BOZ 1160; National Library of Warsaw: Warsaw, Poland, 1733.
11. Zagórski, O. Architekt Kacper Bażanka ok. 1680–1726. *Biul. Hist. Szt.* **1956**, *18*, 84–122.
12. Mączyński, J. *Pamiętnik z Krakowa: Opis tego Miasta i Jego Okolic, Z Rycinami i Planami*; J. Czech: Kraków, Poland, 1845; pp. 342–349.
13. Gubarzewski, K. Notatki dotyczące kościoła i klasztoru xx. pijarów w Krakowie (od roku 1858), Kraków 1910. In *Odbudowa Polskiej Prowincji Pijarów, Działalność Wychowawczo-Edukacyjna Zakonu w Latach 1873–1918*; Ausz, M., Ed.; Wydawnictwo Uniwersytetu Marii Curie-Skłodowskiej: Lublin, Poland, 2013; pp. 228–234.
14. Cempla-Dziadoń, E. *Program prac Konserwatorskich dla Wystroju Malarskiego w Kościele Dolnym—Krypcie Kościoła pw. Przemienienia Pańskiego oo. Pijarów w Krakowie*; No.: 57573; Zbiory Archiwum Wojewódzkiego Urzędu Ochrony Zabytków: Kraków, Poland, 2013; p. 37.
15. Pruszcz, P.H. *Kleynoty Stołecznego Miasta Krakowa, albo Koscioły, y co w Nich Jest Widzenia Godnego y Znącznego, Przez Piotra Hiacyntha Pruszcza, Krotko Opisane, Powtornie zaś z Pilnością Przejrzżane, y do Druku z Additamentem Nowych Kościołow y Relikwii S. Podane, z Pozwoleniem Zwierzchności Duchowney, w Krakowie w Drukarni Akademickiej*; Drukarnia Akademii Krakowskiej: Kraków, Poland, 1745; pp. 43–46.
16. *Resignatio Rectoratus Domus Cracoviensis, Resignatio Fulgencjusza Guttetera 1759 16.VI.* Warsaw; No.: BOZ 1160; National Library of Warsaw: Warsaw, Poland, 1759.
17. Bertolucci, M. *Instruction Relics in the Church: Authenticity and Preservation*; Congregation for the causes of saints: Rome, Italy, 2017; Available online: [https://www.vatican.va/roman\\_curia/congregations/csaints/documents/rc\\_con\\_csaints\\_doc\\_20171208\\_istruzione-reliquie\\_en.html](https://www.vatican.va/roman_curia/congregations/csaints/documents/rc_con_csaints_doc_20171208_istruzione-reliquie_en.html) (accessed on 15 March 2021).
18. Koziana-Biało, H.; Pachuta, K. *Dokumentacja Powykonawcza Prac Przeprowadzonych w Latach 2017–2020, PRACE Konserwatorskie Przy Wybranych Elementach Wystroju i Wyposażenia Dolnego Kościoła, Zespół Klasztorny OO. Pijarów Przy ul. Pijarskiej 2 w Krakowie*; (Firma Konserwatorska Piotr Biało Zabytki Malarstwa, Rzeźby, Architektury Sp. z o. o.); No.: 77941; Zbiory Archiwum Wojewódzkiego Urzędu Ochrony Zabytków Krakowa: Kraków, Poland, 2021; Volume 1, p. 201.
19. Chukanov, N.V.; Viganasina, M.F. *Vibrational (Infrared and Raman) Spectra of Minerals and Related Compounds*; Springer: Cham, Switzerland, 2020; p. 1376. [\[CrossRef\]](#)
20. Koleini, F.; Colomban, P.; Pikiyayi, I.; Prinsloo, L.C. Glass Beads, Markers of Ancient Trade in Sub-Saharan Africa: Methodology, State of the Art and Perspectives. *Heritage* **2019**, *2*, 2343–2369. [\[CrossRef\]](#)
21. Sodo, A.; Casanova Munichia, A.; Barucca, S.; Bellatreccia, F.; Della Ventura, G.; Butini, F.; Ricci, M.A. Raman, FT-IR and XRD investigation of natural opals. *J. Raman Spectrosc.* **2016**, *47*, 1444–1451. [\[CrossRef\]](#)
22. Curtis, N.J.; Gascooke, J.R.; Johnston, M.R.; Pring, A. A Review of the Classification of Opal with Reference to Recent New Localities. *Minerals* **2019**, *9*, 299. [\[CrossRef\]](#)
23. Barańska, H.; Łabudzińska, A.; Terpiński, J. *Laserowa Spektroskopia Ramanowska. Zastosowanie Analityczne*; Państwowe Wydawnictwo Naukowe: Warszawa, Poland, 1981; p. 225.
24. Tournié, A.; Prinsloo, L.C.; Colomban, P. Raman Spectra Database of the Glass Beads Excavated on Mapungubwe Hill and k2, Two Archaeological Sites in South Africa. 2010. Available online: <https://arXiv:1012.1465> (accessed on 10 April 2021).
25. Koleini, F.; Prinsloo, L.C.; Biemond, W.; Colomban, P.; Ngo, A.; Boeyens, J.C.A.; van der Ryste, M.M.; van Brakel, K. Unravelling the glass trade bead sequence from Magoro Hill, South Africa: Separating pre-seventeenth-century Asian imports from later European counterparts. *Herit. Sci.* **2016**, *4*, 43. [\[CrossRef\]](#)
26. Sachanbiński, M.; Girulski, R.; Bobak, D.; Łydźba-Kopczyńska, B. Prehistoric rock crystal artefacts from Lower Silesia (Poland). *J. Raman Spectrosc.* **2008**, *39*, 1012–1017. [\[CrossRef\]](#)
27. Goldstein, J.; Newbury, D.E.; Echlin, P.; Joy, D.C.; Lyman, C.E.; Lifshin, E.; Sawyer, L.; Michael, J.R. *Scanning Electron Microscopy & X-ray Microanalysis*, 3rd ed.; Kiever Academic/Plenum Publishers: New York, NY, USA, 2003; p. 675.

28. Gratuze, B. Provenance Analysis of Glass Artefacts. In *Modern Methods for Analysing Archaeological and Historical Glass*, 1st ed.; Janssens, K., Ed.; John Wiley & Sons, Ltd.: Hoboken, NJ, USA, 2013; pp. 311–343.
29. Goffer, Z. *Archaeological Chemistry*, 2nd ed.; John Wiley & Sons, Ltd.: Hoboken, NJ, USA, 2007; p. 603.
30. Moretti, C.; Hreglich, S. Raw materials, recipes and procedures used for glass making. In *Modern Methods for Analysing Archaeological and Historical Glass*, 1st ed.; Janssens, K., Ed.; John Wiley & Sons, Ltd.: Hoboken, NJ, USA, 2013; pp. 23–47.
31. Costa, M.; Barrulas, P.; Dias, L.; da Conceição Lopes, M.; Barreira, J.; Clist, B.; Karklins, K.; da Piedade de Jesush, M.; da Silva Domingos, S.; Vandenabeele, P.; et al. Multi analytical approach to the study of the European glass beads found in the tombs of Kulumbimbi (Mbanza Kongo, Angola). *Microchem. J.* **2019**, *149*, 1–13. [[CrossRef](#)]
32. Bronk, H.; Röhrs, S.; Bjeoumikhov, A.; Langhoff, N.; Schmalz, J.; Wedell, R.; Gorny, H.E.; Herold, A.; Waldschläger, U. ArtTAX a new mobile spectrometer for energy-dispersive micro X-ray fluorescence spectrometry on art and archaeological objects. *Fresenius J. Anal. Chem.* **2001**, *371*, 307–316. [[CrossRef](#)]
33. Koleini, F.; Prinsloo, L.C.; Biemond, W.M.; Colomban, P.; Ngo, N.; Boeyens, J.C.A.; van der Ryst, M.M. Towards refining the classification of glass trade beads imported into Southern Africa from the 8th to the 16th century AD. *J. Cult. Herit.* **2016**, *19*, 435–444. [[CrossRef](#)]
34. Cagno, S.; Favaretto, L.; Mendera, M.; Izmer, A.; Vanhaecke, F.; Janssens, K. Evidence of early medieval soda ash glass in the archaeological site of san Genesio (Tuscany). *J. Archaeol. Sci.* **2012**, *39*, 1540–1552. [[CrossRef](#)]
35. Cagno, S.; Cosyns, P.; Izmer, A.; Vanhaecke, F.; Nysc, K.; Janssens, K. Deeply colored and black-appearing Roman glass: A continued research. *J. Archaeol. Sci.* **2014**, *42*, 128–139. [[CrossRef](#)]
36. Baert, K.; Meulebroeck, W.; Ceglia, A.; Wouters, H.; Cosyns, P.; Nys, K.; Thienpont, H.; Terry, H. The potential of Raman spectroscopy in glass studies. In Proceedings of the SPIE 8422, Integrated Approaches to the Study of Historical Glass, Brussels, Belgium, 7 November 2012; p. 842207. [[CrossRef](#)]
37. Dussubieux, L.; Kusimba, C.; Gogte, V.; Kusimba, S.B.; Gratuze, B.; Oka, R. The trading of ancient glass beads: New analytical data from south Asian and east African soda–alumina glass beads. *Archaeometry* **2008**, *50*, 797–821. [[CrossRef](#)]
38. Stern, W.B.; Gerber, Y. Potassium-Calcium Glass: New data and experiments. *Archaeometry* **2004**, *46*, 137–156. [[CrossRef](#)]
39. Greiner-Wronowa, E. *The Archaeometry of Historical Glass*; Wyd. AGH: Kraków, Poland, 2017; p. 265.
40. Morozova, E.A.; Kadikova, I.F.; Yuryeva, T.V.; Yuryev, V.A. Crystallites in color glass beads of the 19th century and their influence on fatal deterioration of glass. In Proceedings of the Advances in Applied Physics and Materials Science Congress & Exhibition, Mugla, Turkey, 22–26 April 2017; Available online: <https://arxiv.org/abs/1705.08330> (accessed on 10 April 2021).
41. Pankiewicz, A.; Siemianowska, S.; Sadowski, K. Wczesnośredniowieczna biżuteria szklana z głównych ośrodków grodowych Śląska (Wrocław, Opole, Niemcza). In *Pago Silensi, Wrocławskie Studia Wczesnośredniowieczne 3*; Uniwersytet Wrocławski: Wrocław, Poland, 2017; p. 364. [[CrossRef](#)]
42. Mimoso, J.M. Origin, early history and technology of the blue pigment in azulejos. In Proceedings of the GlazeArch 2015 International Conference Glazed Ceramics in Architectural Heritage, Lisbon, Portugal, 2–3 July 2015; pp. 357–375. Available online: [http://azulejos.lnec.pt/AzuRe/links/07%20Origin\\_of\\_blue\\_pigment.pdf](http://azulejos.lnec.pt/AzuRe/links/07%20Origin_of_blue_pigment.pdf) (accessed on 10 April 2021).
43. Dussubieux, L.; Gratuze, B. Chemical Composition of 16th- to 18th-Century Glass Beads Excavated in Paris. *BEADS J. Soc. Bead Res.* **2012**, *24*, 26–38. Available online: <https://surface.syr.edu/beads/vol24/iss1/6> (accessed on 15 May 2021).
44. Żelechower, M.; Stróż, D.; Ryba-Romanowski, W. Wybrane metody badań materiałów. Available online: <https://delibra.bg.polsl.pl/publication/36930> (accessed on 15 April 2021).
45. Caggiani, M.C.; Acquafredda, P.; Colomban, P.; Mangone, A. The source of blue colour of archaeological glass and glazes: The Raman spectroscopy/SEM-EDS answers. *J. Raman Spectrosc.* **2014**, *45*, 1251–1259. [[CrossRef](#)]
46. Colomban, P. The destructive/non-destructive identification of enameled pottery, glass artifacts and associated pigments—A brief overview. *Arts* **2013**, *2*, 77–110. [[CrossRef](#)]
47. Colomban, P. Rocks as blue, green and black pigments/dyes of glazed pottery and enameled glass artefacts—A review. *Eur. J. Mineral.* **2014**, *25*, 863–879. [[CrossRef](#)]
48. Gratuze, B.; Pactat, I.; Schibille, N. Changes in the Signature of Cobalt Colorants in Late Antique and Early Islamic Glass Production. *Minerals* **2018**, *8*, 225. [[CrossRef](#)]
49. Beard, J.S.; Tracy, R.J. Spinels and other oxides in Mn-rich rocks from the Hutter Mine, Pittsylvania County, Virginia, USA with implications for solvus relations among jacobsite, galaxite, and magnetite. *Am. Mineral.* **2002**, *87*, 690–698. [[CrossRef](#)]
50. Siddall, R. Mineral pigments in archaeology: Their analysis and the range of available materials. *Minerals* **2018**, *8*, 201. [[CrossRef](#)]
51. Tzankova, N.; Mihaylov, P. Chemical characterization of glass beads from the necropolis of Dren-Delyan (6th–4th century BC), Southwest Bulgaria. *Geol. Balc.* **2019**, *48*, 31–50.
52. Klein, H.A. Eastern Objects and Western Desires: Relics and Reliquaries between Byzantium and the West. *Dumbarton Oaks Papers.* **2004**, *58*, 283–314. [[CrossRef](#)]
53. Teteriatnikov, N. The True Cross Flanked by Constantine and Helena. A Study in the Light of the Post-Iconoclastic Re-evaluation of the Cross. *Delt. Tes Khristianikes Archaologikes Hetaireias* **1995**, *18*, 169–199. [[CrossRef](#)]
54. Pallottini, E. The Epigraphic Presence on the Borghorst Cross (c. 1050). In *Sacred Scripture/Sacred Space*; Frese, T., Keil, W.E., Krüger, K., Eds.; De Gruyter: Berlin, Germany; Boston, MA, USA, 2019; pp. 63–84. [[CrossRef](#)]
55. Marecki, J.; Rotter, L. *Relikwie, Historia, cuda, kult, Leksykon*; Wydawnictwo eSPe: Kraków, Poland, 2012; p. 198.

56. Gerevini, S. Christus crystallus. Rock Crystal, Theology and Materiality in the Medieval West. In *Matter of Faith: An Interdisciplinary Study of Relics and Relic Veneration in the Medieval Period*; Robinson Lloyd de Beer, J., Harnden, A., Eds.; The British Museum: London, UK, 2014; pp. 92–99.
57. McEwan, B.G.; Davidson, M.W.; Mitchem, J.M. A Quartz Crystal Cross from Mission San Luis, Florida. *J. Archaeol. Sci.* **1997**, *24*, 529–536. [[CrossRef](#)]
58. Szczepkowska-Naliwajek, K. *Relikwiarze Średniowiecznej Europy od IV do Początku XVI Wieku: Geneza, Treści, Styl i Techniki Wykonania*; Fundacja ATK: Warszawa, Poland, 1996; p. 353.
59. Razzall, S. Reliquary: A box for a relic. In *Boxes: A Field Guide*, 1st ed.; Bauer, S., Schlünder, M., Rentetzi, M., Kismet Bell, J., Brownell, E., Mechler, U., Eds.; Mattering Press: Manchester, UK, 2020; pp. 597–606. [[CrossRef](#)]
60. Wyrobisz, A. *Szkło w Polsce od XIV do XVII w.*; Wydawnictwo Polskiej Akademii Nauk: Wrocław, Poland; Warszawa, Poland; Kraków, Poland, 1968; p. 223.
61. Perego, E. Magic and Ritual in Iron Age Veneto, Italy. *Pap. Inst. Archaeol.* **2010**, *20*, 67–96. [[CrossRef](#)]